Journal of Alloys and Compounds 509 (2011) 5804–5809

Contents lists available at ScienceDirect

Journal of Alloys and Compounds

journal homepage: www.elsevier.com/locate/jallcom

Influence of interstitial and substitutional atoms on the crystal structure of $La(FeSi)_{13}$

L. Jia, J.R. Sun*, J. Shen, B. Gao, T.Y. Zhao, H.W. Zhang, F.X. Hu, B.G. Shen

State Key Laboratory for Magnetism, Institute of physics & Center for Condensed Matter Physics, Chinese Academy of Sciences, Beijing 100080, PR China

ARTICLE INFO

Article history:
Received 8 December 2010
Received in revised form 20 February 2011
Accepted 22 February 2011
Available online 1 March 2011

PACS:
75.30.Sg
65.40.Gr
75.30.Kz

Keywords:
Substitution
Lattice expansion
Interstitial atoms
Fe–Fe bond

ABSTRACT

The influence of interstitial hydrogen or carbon on the crystal structure of $LaFe_{11.5}Si_{1.5}H_\delta$ (δ = 0, 1.2, and 2) and $LaFe_{11.5}Si_{1.5}C_\delta$ (δ = 0, 0.1, 0.2, 0.3, 0.4, and 0.5) has been investigated based on the Rietveld analyses of powder X-ray diffraction spectra. Effects of Ce substitution for La are also studied for comparison. The incorporation of interstitial atoms causes a lattice expansion of the compounds while leaves the structural symmetry unchanged. Accompanying the lattice expansion, Fe–Fe bond exhibits a concomitant variation. Four of the five Fe–Fe bonds show a tendency to expansion. The largest elongation occurs for the shortest inter-cluster bond, and the relative change is as large as ~2.53% as δ increases from 0 to 2 for $LaFe_{11.5}Si_{1.5}H_\delta$. In contrast, the longest Fe–Fe bond shrinks considerably (−0.97%). Similarly effects on Fe–Fe bonds are produced by the paramagnetic to ferromagnetic transition, though the bond variation is smaller. Increase in Ce content produces, fascinatingly, essentially the same effects as the decrease of interstitial content, though Ce occupies different crystallographic sites than those occupied by interstitial atoms. Influence of interstitial atoms on magnetic behaviors may be dominated by the change of the shortest Fe–Fe bond.

1. Introduction

Recently, giant magnetocaloric effect (MCE) has been observed in the materials such as $Gd_5(Si_xGe_{1-x})_4$ [1], $La(Fe, M)_{13}$ (M = Si, Al, Co) [2–6], MnAs [7] and $MnFeP_{1-x}As_x$ [8], which experience a first-order phase transition. The typical entropy change for the field change of 0–5 T is ~20 J/kgK for $LaFe_{13-x}M_x$ (M = Si, Co) [2,3,6] near the ambient temperature. This is a value nearly double that of Gd (~10 J/kg K), which has been regarded as the most promising refrigerant for room-temperature magnetic cooling. These discoveries demonstrate a possibility to apply the magnetic cooling technique, which has significant advantages over the conventional refrigeration technique, near the ambient temperature [9].

Among the MCE materials, $LaFe_{13-x}Si_x$ is of special interest. In addition to giant MCE, the most remarkable feature of $LaFe_{13-x}Si_x$ is the strong dependence of its Curie temperature (T_C) on element doping or external perturbations such as magnetic field and pressure. It has been reported that a pressure of 1 GPa reduces T_C by ~100 K [10], whereas a magnetic field of 5 T upwards shifts T_C by ~25 K [11], as a result of the field-induced itinerant-electron metamagnetic transition. Compared with magnetic field and pressure, effects of interstitial atoms such as hydrogen and carbon are much stronger, and the incorporation of δ = 1.5 hydrogen in $LaFe_{11.44}Si_{1.56}H_\delta$ can lift T_C by ~130 K [11,12]. What is of special interest is that the phase transition of the hydride remains to be first-order in nature despite the great increase of T_C [11–13]. This is in sharp contrast to the effect of Si or Co doping, which increases Curie temperature while driving the transition from first order to second order [14–16]. In addition to this, $La(Fe, M)_{13}$ also exhibits diverse magnetic structures such as antiferromagnetic (AFM) order and spin glass-like structure when Fe is partially replaced by Al [17] and Mn [18], respectively. All these results reveal the complexity of the mechanism that governs the magnetic coupling in this kind of compounds.

It has been reported that the magnetic interaction in RE–Fe-based compounds (RE = rare earth) is predominantly determined by Fe–Fe and RE–Fe interactions [19]. A relation between the Fe–Fe exchange integral and the Fe–Fe separation has been established by Li and Morrish for the $Sm_2Fe_{17}N_\delta$ compound based on the analyses of Mössbauer spectra [20]. It was found that the magnetic interaction is AFM when the Fe–Fe distance is smaller than ~2.45 Å, while ferromagnetic (FM) above ~2.45 Å. A remarkable result is the crucial dependence of Fe–Fe exchange on atomic separation: The exchange integral is negative and grows steeply as the Fe–Fe distance approaches 2.45 Å from below. This actually implies the possibility to modify the Curie temperature by tuning Fe–Fe distance.

Compared with $Sm_2Fe_{17}N_\delta$, the exchange interaction in $LaFe_{13-x}Si_x$ exists mainly between Fe atoms [21]. The Fe–Fe inter-

* Corresponding author. Tel.: +86 10 82648075; fax: +86 10 82649485.
E-mail address: jrsun@g203.iphy.ac.cn (J.R. Sun).

0925-8388/$ – see front matter © 2011 Elsevier B.V. All rights reserved.
doi:10.1016/j.jallcom.2011.02.124

action could depend crucially on Fe–Fe distance as occurred in $Sm_2Fe_{17}N_\delta$. External disturbances such as interstitial atom and high pressure affect the magnetic behaviors by modifying Fe–Fe bonds. Although the atomic structure of $LaFe_{13-x}Si_x$ with different Si content and/or interstitial H atoms has been studied before [22], there are no systematical reports about the structure deformations produced by the amount of interstitial atoms and partial replacement of La by smaller rare-earths. It is therefore necessary to establish a clear picture about how atomic structure changes with the help of the X-ray diffraction (XRD) technique. This could be helpful to find out the key factors that govern the magnetic coupling in the compound. Based on this consideration, in this paper we performed a comprehensive study on the atomic structure of the $LaFe_{13-x}Si_x$ compounds with or without interstitial atoms based on the Rietveld analyses of the powder XRD spectra. Effects of Ce substitution for La are also studied for comparison.

2. Experimental procedures

The $LaFe_{11.5}Si_{1.5}$ compound was prepared by arc melting appropriate amounts of starting materials (99.9% or higher in purity) under argon atmosphere (~10 at% excessive La was used to compensate the weight loss during the arc melting). The resultant ingots were first annealed at 1323 K for 50 days in an evacuated quartz tube, to improve both the phase purity and the crystallization, then quenched into liquid nitrogen. We used an intermediate Fe–C alloy, for which the content of C is known, as one of the starting materials for the preparation of the carbon-doped alloys. By adjusting the proportion of Fe–C, the C content was controlled. To get the corresponding hydrides, the $LaFe_{11.5}Si_{1.5}$ alloy was first fully hydrogenated in a H_2 atmosphere of 5 MPa at 423 K for ~5 h, then annealed in high vacuum ($\sim 5 \times 10^{-4}$ Pa) at 523 K for different durations to control the release of hydrogen. The content of hydrogen in the sample was determined by comparing the Curie temperature of $LaFe_{11.5}Si_{1.5}H_\delta$ with that of a similar compound $LaFe_{11.44}Si_{1.56}H_\delta$, for which δ has been explicitly given [11]. The $LaFe_{11.5}Si_{1.5}C_\delta$ carbides for $\delta = 0$, 0.1, 0.2, 0.3, 0.4 and 0.5 were synthesized following the same procedure as that for the $LaFe_{11.5}Si_{1.5}$ compound except for the use of an appropriate amount of Fe–C alloy as starting material. Specimens with partially replaced La by Ce, $La_{1-x}Ce_xFe_{11.5}Si_{1.5}$ for $x = 0.1$, 0.2, 0.3, and 0.4, were also prepared for a comparison study.

Powder X-ray diffraction (XRD) data were recorded by a Rigaku D/max-2400 diffractometer with a rotating anode and the Cu $K\alpha$ radiation. A graphite monochromator has been employed in the diffractometer to get ride of fluorescent radiation due to the absorption of Cu $K\alpha$ radiation by Fe. Data were collected over the 2θ range of 20–120°, with the step size of 0.02° for the 2θ-scan and the duration of 2 s/step for data recording, were analyzed by the Rietveld refinement via the program FULLPROF [23].

3. Results and discussion

3.1. General structural changes

Energy dispersive analysis of X-ray (EDX) indicates that the atomic percentages of La, Fe and Si are 6.04%, 84.47% and 9.47% for the $LaFe_{11.5}Si_{1.5}$ compound, close to the designed compositions (La: 7.14%, Fe: 82.14% and Si: 10.72% for $LaFe_{11.5}Si_{1.5}$) considering the uncertainty (~3%) of EDX. XRD data indicate that clean single-phase samples were obtained. The diffraction peaks are sharp and can be indexed based on the cubic $NaZn_{13}$-type structure. The introduction of interstitial hydrogen or carbon causes a lattice expansion as demonstrated by the low-angle shift of XRD peaks, while the sample remains to be single phase. To get the knowledge about atomic structure, a Rietveld refinement of the XRD data was further performed based on the space group $Fm\bar{3}c$. It has been evidenced that interstitial atoms do not affect the symmetry of the samples [24]. As revealed by previous work for $LaFe_{10.9}Al_{2.1}$ [24] and $LaFe_{11.31}Si_{1.69}$ [22], there are two different crystal sites for Fe, namely Fe^{I} and Fe^{II}, representing the Fe atoms at the center and on the surface of the $(Fe/Si)_{13}$ icosahedral cluster, respectively. Si atoms are assumed to randomly replace Fe^{II}. Different from this result, for $LaFe_{11.4}Si_{1.6}$ [25], Wang et al. found that Si distributes randomly in both the 8b and 96i sites. In this work, we accepted the conclusion of Wang et al.

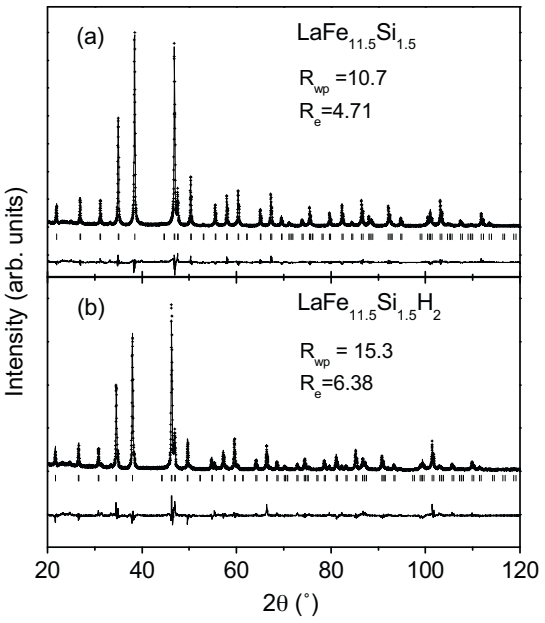

Fig. 1. Observed (crosses) and calculated (solid lines) XRD patterns of the $LaFe_{11.5}Si_{1.5}$ and $LaFe_{11.5}Si_{1.5}H_2$ compounds. The lowest curve shows the difference between observed and calculated patterns. Vertical bars show the positions of Bragg reflections.

Table 1
Atomic position of Fe^{II}, Fe–Fe bond length, lattice constant, and weighted profile R factor of the compounds $LaFe_{11.5}Si_{1.5}H_\delta$ ($\delta = 0$ and 2) and $LaFe_{11.5}Si_{1.5}C_\delta$ ($\delta = 0.5$).

	$LaFe_{11.5}Si_{1.5}$	$LaFe_{11.5}Si_{1.5}H_{2.0}$	$LaFe_{11.5}Si_{1.5}C_{0.5}$
x	0	0	0
y	0.17899 (2)	0.17953 (4)	0.17876 (2)
z	0.11694 (2)	0.11442 (4)	0.11702 (2)
a (Å)	11.4685 (1)	11.6068 (1)	11.5136 (1)
B_1 (Å)	2.4520 (1)	2.4710 (5)	2.4599 (2)
B_2 (Å)	2.6823 (3)	2.6561 (7)	2.6946 (3)
B_3 (Å)	2.5532 (2)	2.5840 (6)	2.5606 (2)
B_4 (Å)	2.4462 (3)	2.5082 (7)	2.4564 (5)
B_5 (Å)	2.5000 (3)	2.4907 (6)	2.5143 (3)
R_{wp} (%)	10.7	15.3	11.5

Fig. 1 shows the observed and calculated XRD patterns for selected samples $LaFe_{11.5}Si_{1.5}H_\delta$ ($\delta = 0$ and 2). A satisfactory agreement is obtained in the whole 2θ range investigated. The deduced atomic parameters, Fe–Fe bonds, and weighted profile R factors are given in Table 1.

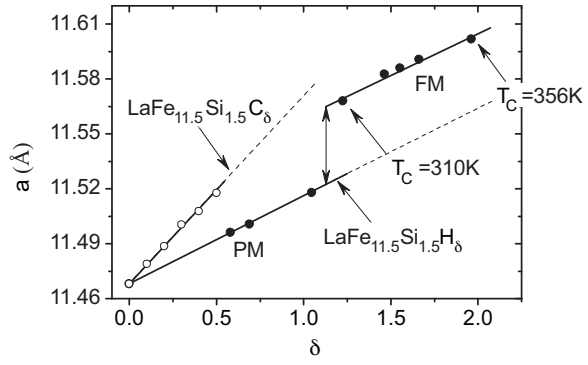

Fig. 2. Lattice constant as a function of the content of interstitial atoms for the $LaFe_{11.5}Si_{1.5}H_\delta$ hydrides and $LaFe_{11.5}Si_{1.5}C_\delta$ carbides. Solid and dashed lines are guides for the eye.

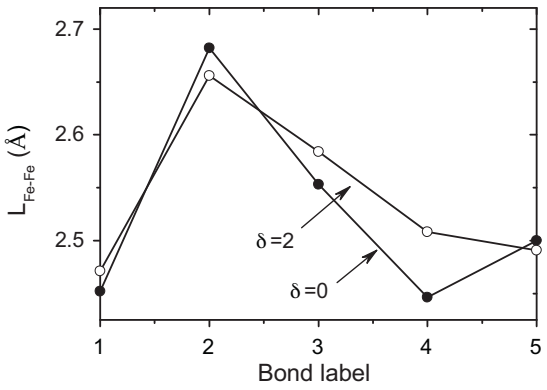

Fig. 3. Change of Fe–Fe bond length upon hydrogenating for the compound $LaFe_{11.5}Si_{1.5}H_\delta$. The arrow marks the expansion of Fe–Fe bond after hydrogen absorption.

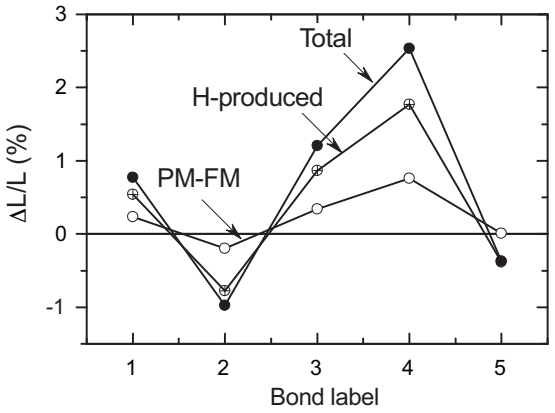

Fig. 4. Relative change of Fe–Fe bonds resulted by the PM–FM transition (marked by PM–FM) and the lattice expansion of the PM phase due to the incorporation of interstitial hydrogen (marked by H-produced) for the compounds $LaFe_{11.5}Si_{1.5}H_2$.

Fig. 2 exemplifies the lattice constant of $LaFe_{11.5}Si_{1.5}H_\delta$ as a function of hydrogen content. a increases linearly with δ in the ranges from $\delta = 0$ to ~1.2 and from ~1.2 to ~2. There is an abrupt jump of lattice constant near $\delta \approx 1.2$, which is a result of the paramagnetic (PM) to FM transition. The XRD was performed at the ambient temperature, and the data obtained are for the PM phase when δ <1.2 and for the FM phase otherwise ($T_C > 296$ K for $\delta > 1.2$). A simple analysis shows the lattice expansion of ~0.044 Å, caused by the magnetic transition regardless of the temperature where the phase transition takes place. In contrast, the relative change of a produced by one percent interstitial atoms is ~0.41% for $LaFe_{11.5}Si_{1.5}H_\delta$, without considering the lattice jump of the magnetic transition, and ~0.9% for $LaFe_{11.5}Si_{1.5}C_\delta$. The effect of carbon is stronger compared with that of hydrogen, which is reasonable noting the large atomic size of carbon. The atomic radius of C is ~1.7 times as large as that of H, while the ratio of the two a–δ slopes is ~2.1.

There are totally five kinds of Fe–Fe bonds (B_1–B_5) within the distance of 2.7 Å for the $LaFe_{11.5}Si_{1.5}$ compound, with the bond lengths of L_{Fe-Fe} = 2.4520 Å, 2.6823 Å, 2.5532 Å, 2.4462 Å, and 2.5000 Å, respectively (Table 1). The first three bonds are formed by the Fe atoms in the same cluster, while the last two in two neighboring clusters. The shortest Fe–Fe bond is B_4, an inter-cluster bond. These results are consistent with those previously reported [22,25].

Accompanying the introduction of H atoms, Fe–Fe bonds exhibit concomitant variations. We selected two hydrides with $\delta = 0$ and 2, which have obviously different lattice parameters, for further analyses. Fig. 3 shows the variation of Fe–Fe bonds upon hydrogenating. Four of the five Fe–Fe bonds show a tendency to expansion. The largest elongation occurs for the shortest inter-cluster bond, and the relative change is ~2.53% as δ increases from 0 to 2. In contrast, the longest bond B_2, one of the intra-cluster bonds, shrinks considerably (−0.97%). The tendency of Fe–Fe bond variation is agreeable with the result obtained in hydride $LaFe_{11.31}Si_{1.69}H_{1.45}$ compound [22]. A simple analysis shows the bond population of B_1:B_2:B_3:B_4:B_5 = 2:1:4:2:2. Therefore, the weighted average of the Fe–Fe bond length can be obtained, and it is found to grow from ~2.5178 Å to ~2.5387 Å for δ from 0 to 2. An interesting result is the considerable reshaping of the $(Fe/Si)_{13}$ icosahedra upon hydrogenating, as revealed by the asynchrony of bond expansion/contraction.

XRD analysis indicates that clean single-phase samples can be obtained when the content of Ce is below ~0.3 and about 12% impurity phases were found when the content of Ce is 0.4. The replacement of La with Ce results in a lattice contraction, while the symmetry of the sample remains unchanged. The lattice constant decreases from 11.4680 Å for $LaFe_{11.5}Si_{1.5}$ to 11.4498 Å for $La_{0.7}Ce_{0.3}Fe_{11.5}Si_{1.5}$. Although the effect is weak, the relative change of the Fe–Fe bond can be reliably determined by the Rietveld analysis of the XRD data. Fascinatingly, increase in Ce content produces essentially the same effects on Fe–Fe bonds as the decrease of interstitial content, though Ce occupies different crystallographic sites from the interstitial atoms.

3.2. Structural change in different processes

It is obvious that the lattice constant of the PM phase undergoes an expansion after the hydrogen absorption, and the T_C increases from below to above the ambient temperature. Therefore, Fig. 3 is a combined effect of the lattice expansion of PM phase due to the incorporation of interstitial atoms and the lattice expansion from the PM to the FM phase. The influence of these two processes on Fe–Fe bonds is distinguishable. To study the structure difference of the PM and FM phases of $LaFe_{11.5}Si_{1.5}H_2$, two sets of XRD data near the temperatures just below and above T_C = 356 K are required. However, a XRD experiment lasting for ~3 h at a temperature above 356 K may cause a hydrogen release, which will affect the reliability of the data. According to Fig. 2, the lattice difference of the PM and FM phases is essentially the same when phase transition takes place in the temperature range, for example, from 300 K to 360 K. This implies that the structure difference of the PM and FM phases of $LaFe_{11.5}Si_{1.5}H_2$ can be approximated by a hydride with a lower Curie temperature, for example, $LaFe_{11.5}Si_{1.5}H_{1.2}$, which exhibits a Curie temperature of T_C ~310 K.

The experiment was performed on the Rigaku diffractometer with a home-made heater that can provide an environment up to the temperature of ~323 K. Two sets of XRD data were recorded at the temperatures of ~296 K and ~323 K, respectively, and analyzed by the Rietveld technique. The difference of the bond lengths of the PM and FM phases are shown in Fig. 4 (marked by PM–FM). Considering the fact that the thermal expansion is negligible when the temperature interval is small, differences of the Fe–Fe bonds obtained at ~296 K and ~323 K, respectively, could be exclusively ascribed to magnetic transition. With the bond elongation associated with the PM to FM transition being known, the expected Fe–Fe bond change simply produced by interstitial hydrogen, without magnetic transition, can be obtained for $LaFe_{11.5}Si_{1.5}H_2$ (marked by H-produced). The total bond changes are also shown for comparison. It is interesting that the effects of interstitial atoms and magnetic transition are similar for B_1, B_3 and B_4, in which bond change due to interstitial atoms is ~2.4 times as large as that produced by magnetic transition ($\delta = 0 \rightarrow 2$) (Fig. 4). The changes of B_5 bonds can be ascribed mostly from the hydrogenation. The contraction of B_2 bond upon the PM–FM transition is a result different

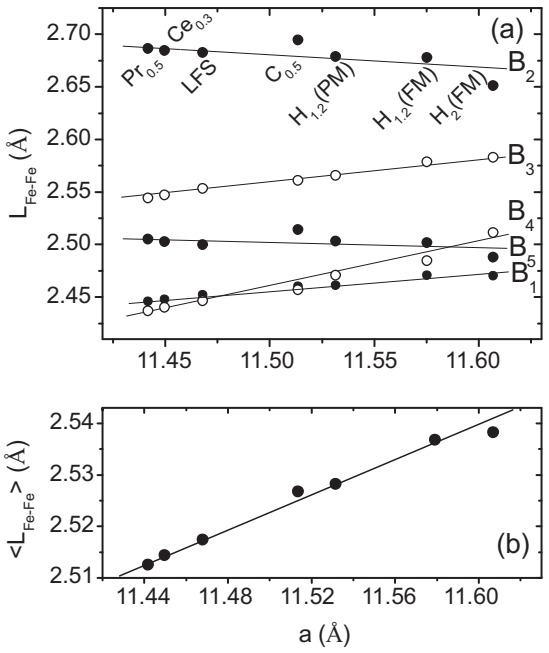

Fig. 5. Bond length (a) and average bond length (b) as functions of lattice constant for $La_{0.7}Ce_{0.3}Fe_{11.5}Si_{1.5}$, $LaFe_{11.5}Si_{1.5}H_\delta$ (δ = 0, 1.2, 2) and $LaFe_{11.5}Si_{1.5}C_{0.5}$ compounds. Results of $La_{0.5}Pr_{0.5}Fe_{11.5}Si_{1.5}$ were also shown for comparison. Solid lines are guides for the eye.

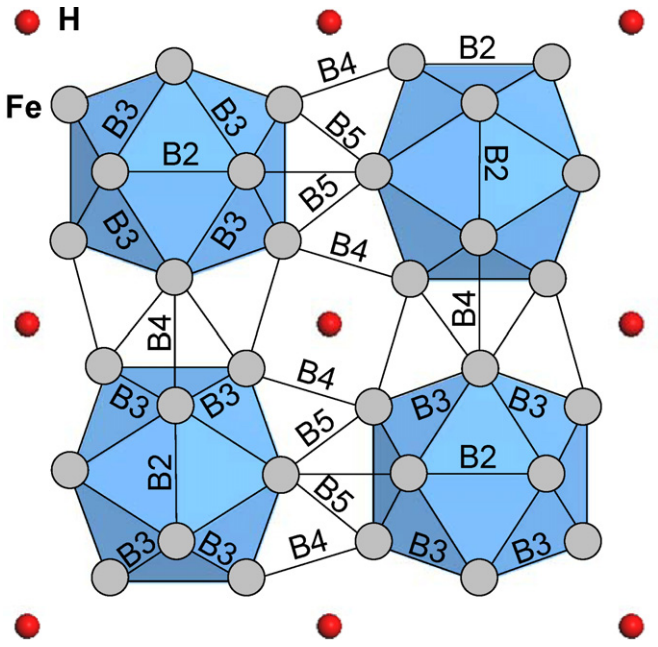

Fig. 6. A schematic diagram for the atomic structure of $LaFe_{13}H_3$ (La is omitted for clarity).

from that of Wang et al. [25] who have studied the atomic structure of $LaFe_{11.4}Si_{1.6}$ based on neutron diffraction, and observed elongations for all of the five Fe–Fe bonds upon the PM–FM transition. The reason for this discrepancy may be the difference of the samples used for the analyses. Different from the hydrogen-free sample used by Wang et al., interstitial hydrogen has distorted the atomic structure of $LaFe_{11.5}Si_{1.5}H_{1.4}$ even in the PM state, causing a contraction of the B_2 bond and an expansion of the B_4 bond.

Fig. 5 shows the bond length as a function of lattice parameter. A linear increase of L_{Fe-Fe} with a is observed for four of the five bonds, at the rate of 0.1554 for B_1, 0.2346 for B_3, 0.4164 for B_4. In contrast, the longest bond B_2 and inter-cluster bond B_5 exhibit a slight decrease at the rate of −0.1513 and −0.061 with lattice constant. The weighted average of the Fe–Fe bond length is 2.512 Å, and it increases at a rate of ∼0.175 with increasing a. These results are important in the sense that they reveal the one-to-one correspondence between lattice parameter and the Fe–Fe bond, regardless of the origins for the lattice variation: the structure change can caused by the incorporation of interstitial atoms, by magnetic transition, or by the replacement of La by other rare-earths. Based on Fig. 4, changes in Fe–Fe bonds can be readily deduced from those of lattice parameter.

Fig. 6 is a schematic diagram showing the atomic structure of $LaFe_{11.5}Si_{1.5}H_3$ (La is omitted for clarity). There are eight Fe–Fe bonds, four B_4 bonds and four B_5 bonds, between two adjacent $(Fe/Si)_{13}$ icosahedra (only three B_4 bonds and two B_5 bonds on the top can be seen in the figure). The interstitial site locates at the space caged by four adjacent icosahedra lying in the same plane, encircled by four B_4 bonds. This explains the expansion of B_4 as interstitial atoms are introduced. Change of other bonds is indirect, as a cooperative structure deformation to accommodate the interstitial atoms. Different from hydrogen and carbon, La situates in the center of space caged by eight adjacent icosahedra. It is obvious that replacing La with smaller rare-earths may directly affect the B_4 bond also. Therefore, the effects on structure of introducing small rare-earths and decreasing interstitial content could be exactly the same.

3.3. Magnetic properties

To get a deep insight into the underlying physics of volume effects, it would be helpful to study the relation between a and T_C, which is an approximate measure of the magnetic coupling in compounds. Fig. 7 exemplifies the temperature-dependent magnetization (M) of selected samples $La_{0.7}Ce_{0.3}Fe_{11.5}Si_{1.5}$, $LaFe_{11.5}Si_{1.5}H_\delta$ (δ = 0, 1.5, and 2) and $LaFe_{11.5}Si_{1.5}C_{0.4}$ measured under the field of 0.05 T. A clear magnetization change is observed around T_C (the turning point of the M–T curve), and further analyses of the M-magnetic field relations reveal the first-order character of the phase transition. The strong effect of interstitial hydrogen can be identified from the obvious shift of T_C with δ. T_C is ∼194 K for $LaFe_{11.5}Si_{1.5}$, goes up rapidly with the content of hydrogen increases, and arrives ∼356 K when $\delta \approx 2$. These results are consistent with those obtained by Fujita et al. in $LaFe_{11.44}Si_{1.56}H_\delta$ system [11]. The incorporation of δ = 0.5 carbon increases the Curie temperature by ∼46 K. In addition, the substitution of Ce for 30% La leads a decrease of ∼26 K for T_C. Different from the changes of T_C, the saturation magnetization (the magnetic moment of Fe) is almost unaffected by the incorporation of interstitial atoms or Ce [11,26].

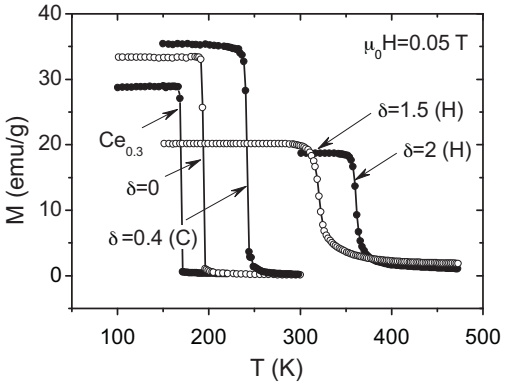

Fig. 7. Temperature dependence of magnetization measured under the field of 0.05 T for the $La_{0.7}Ce_{0.3}Fe_{11.5}Si_{1.5}$, $LaFe_{11.5}Si_{1.5}H_\delta$ (δ = 0, 1.5, and 2.0) and $LaFe_{1.5}Si_{1.5}C_\delta$ (δ = 0.4) compounds.

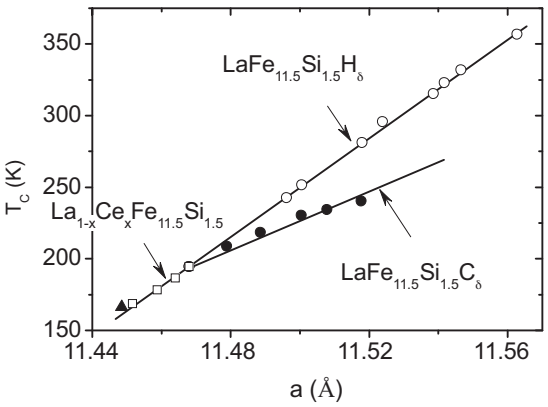

Fig. 8. Curie temperature as a function of lattice constant for the $La_{1-x}Ce_xFe_{11.5}Si_{1.5}$ (x = 0–0.3) $LaFe_{11.5}Si_{1.5}H_\delta$ (δ = 0–2) and $LaFe_{1.5}Si_{1.5}C_\delta$ (δ = 0–0.5) compounds. Triangle represents the data of $La_{0.6}Ce_{0.4}Fe_{11.5}Si_{1.5}$ compound which deviates from the linearity could be a result of the appearance of impurity phases in this compound. Solid lines are guides for the eye.

Fig. 8 shows the Curie temperature as a function of lattice constant. A linear increase of T_C with a at a rate of ~1779 K/Å is observed for $LaFe_{11.5}Si_{1.5}H_\delta$ and $La_{1-x}Ce_xFe_{11.5}Si_{1.5}$, where $a = a_0$ for $T_C < 296$ K and $a = a_0 - \Delta a$ for $T_C > 296$ K, a_0 is the lattice constant at the room temperature, $\Delta a \approx 0.044$ Å is the change of lattice constant corresponding to the FM–PM transition. From our previous study, RE–Fe coupling in $R_{1-x}La_xFe_{11.5}Si_{1.5}$ (R = Ce, Pr, Nd) is different, which leads to different slopes of T_C–a relations [21]. Meanwhile, the introduction of carbon leads to an increase of T_C at a rate of ~1089 K/Å. The tendency is clear: T_C increases as lattice expands or, equivalently, Fe–Fe distance increases.

A recent study about the influence of interstitial H on the electron structure for $La(Fe_{0.88}Si_{0.12})_{13}H_{1.6}$ compound by Mössbauer spectroscopy indicates the valence electron transfer from hydrogen to Fe is negligible small, which means the magnetic coupling is closely associated with a volume expansion after hydrogenation [27]. It was also found that high pressure and hydrogenising produce exactly the opposite effect, suggesting the unimportance of the electronic process [28]. According to Givord et al. [19], the Fe–Fe interaction is an important factor affecting the magnetic behavior of RE–Fe compounds. It was found that the magnetic interaction is AFM when the Fe–Fe distance is smaller than ~2.45 Å, while ferromagnetic (FM) above ~2.45 Å. A remarkable result is the crucial dependence of Fe–Fe exchange on atomic separation: The exchange integral is negative and grows steeply as the Fe–Fe distance approaches 2.45 Å. This actually implies the possibility to modify the Curie temperature by tuning Fe–Fe distance.

In $Sm_2Fe_{17}N_\delta$ compounds, the negative exchange interactions of the Fe–Fe bonds shorter than 2.45 Å govern the Curie temperature. After introducing interstitial N into Sm_2Fe_{17} compounds, the exchange integrals of the short Fe–Fe bonds increase due to the lattice expansion, thus it enhances T_C significantly. Considering the fact that the main element of $LaFe_{13-x}Si_xH_\delta$ and $Sm_2Fe_{17}N_\delta$ is Fe, similar process may take place in the lattice of $LaFe_{13-x}Si_xH_\delta$. It is found that three kinds of bonds elongation after hydrogenising and the largest elongation takes place in B_4, the only bond shorter than 2.45 Å in $LaFe_{11.5}Si_{1.5}$. On the knowledge of Sm_2Fe_{17}, this expansion may increase the positive exchange integral and B_4 bonds may play an important role in the T_C increasing.

Different from the case of interstitial atoms, increasing Si content in $LaFe_{13-x}Si_x$ (x from 1.6 to 2.6) would decrease the lattice volume, while it also leads to an increase of the Curie temperature. It should be emphasized that the bond length of B_1 increases while the lattice contracts with Si content increasing. Therefore, positive exchange interaction enhances as a result of the length of B_1 increasing, which contributes to the magnetic exchange interaction mostly [29]. Although the difference of atomic structure between the $LaFe_{13-x}Si_x$ and its hydrides is obviously, the increases of T_C are all originated from the enhancement of positive exchange integral due to the elongation of Fe–Fe bond.

From above analysis, the Fe–Fe distance affects the T_C definitely, but there is a considerable discrepancy between the T_C–a relations of $LaFe_{11.5}Si_{1.5}H_\delta$ and $LaFe_{11.5}Si_{1.5}C_\delta$. The T_C–a slope of the former is significantly larger than that of the latter. A possible explanation may be the occurrence of a complex process, for example, charge transferring between Fe and C in the carbides. The presence of minor secondary phase in the carbides can affect the composition of the matrix phase and maybe a reason for the slightly deviation from the linearity of T_C–a relation.

4. Summary

The structures of $LaFe_{11.5}Si_{1.5}H_\delta$ (δ = 0, 1.4, and 2), $LaFe_{11.5}Si_{1.5}C_\delta$ (δ = 0, 0.1, 0.2, 0.3, 0.4, and 0.5), and $La_{1-x}Ce_xFe_{11.5}Si_{1.5}$ (x = 0.1, 0.2, 0.3, and 0.4) have been investigated based on the Rietveld analyses of powder X-ray diffraction spectra. Special attention has been paid to the relation between structural and magnetic interplay to find out the key factors that govern the magnetic coupling. The incorporation of interstitial atoms is found to cause a lattice expansion of the compounds while leaves the structure symmetry unaffected. Accompanying the lattice expansion, Fe–Fe bond exhibits a concomitant variation. Four of the five Fe–Fe bonds show a tendency to expansion. The largest elongation occurs for the shortest intercluster bond, and the relative change is as large as ~2.37% as δ increases from 0 to 2 for $LaFe_{11.5}Si_{1.5}H_\delta$. In contrast, the longest Fe–Fe bond, one of the intra-cluster bonds, shrinks considerably (−0.53%). This result indicates a reshaping of the $(Fe/Si)_{13}$ icosahedra upon hydrogenating. Similarly effects on Fe–Fe bonds are produced by the paramagnetic to ferromagnetic transition except that the bond variation is small. Fascinatingly, increase in Ce content produces essentially the same effects on Fe–Fe bonds as the decrease of interstitial content, though interstitial atoms occupy different crystallographic sites from rare-earths. There is a universal relation between Fe–Fe bond length and lattice constant, the former varies linearly with the latter, regardless of the origins for the lattice change. Influence of interstitial atoms on magnetic behaviors may be dominated by the change of the shortest Fe–Fe bond.

Acknowledgements

This work has been supported by the National Natural Science Foundation of China and the National Basic Research of China.

References

[1] V.K. Pecharsky, K.A. Gschneidner Jr., Phys. Rev. Lett. 78 (1997) 4494.
[2] F.X. Hu, B.G. Shen, J.R. Sun, Z.H. Cheng, G.H. Rao, X.X. Zhang, Appl. Phys. Lett. 78 (2001) 3675.
[3] S. Fujieda, A. Fujita, K. Fukamichi, Appl. Phys. Lett. 81 (2002) 1276.
[4] F.X. Hu, B.G. Shen, J.R. Sun, A.B. Pakhomov, C.Y. Wong, X.X. Zhang, S.Y. Zhang, G.J. Wang, Z.H. Cheng, IEEE Trans. Magn. 37 (2001) 2328.
[5] F.X. Hu, B.G. Shen, J.R. Sun, Z.H. Cheng, X.X. Zhang, J. Phys.: Condens. Matter 12 (2000) L691.
[6] F.X. Hu, B.G. Shen, J.R. Sun, G.J. Wang, Z.H. Cheng, Appl. Phys. Lett. 80 (2002) 826.
[7] H. Wada, Y. Tanabe, Appl. Phys. Lett. 79 (2001) 3302.
[8] O. Tegus, E. Bruck, K.H.J. Buschow, F.R. de Boer, Nature 415 (2002) 150.
[9] V.K. Pecharsky, K.A. Gschneidner Jr., J. Magn. Magn. Mater. 200 (1999) 44.
[10] A. Fujita, S. Fujieda, K. Fukamichi, H. Mitamura, T. Goto, Phys. Rev. B 65 (2001) 014410.
[11] A. Fujita, S. Fujieda, Y. Hasegawa, K. Fukamichi, Phys. Rev. B 67 (2003) 104416.
[12] Y.F. Chen, F. Wang, B.G. Shen, J.R. Sun, G.J. Wang, F.X. Hu, Z.H. Cheng, T. Zhu, J. Appl. Phys. 93 (2003) 6981.

[13] J. Lyubina, O. Gutfleisch, M.D. Kuz'min, M. Richter, J. Magn. Magn. Mater. 320 (2008) 2252.
[14] F.X. Hu, X.L. Qian, J.R. Sun, G.J. Wang, X.X. Zhang, Z.H. Cheng, B.G. Shen, J. Appl. Phys. 92 (2002) 3620.
[15] A. Fujita, K. Fukamichi, IEEE Trans. Magn. 35 (1999) 3796.
[16] A. Fujita, Y. Akamatsu, K. Fukamichi, J. Appl. Phys. 85 (1999) 4756.
[17] T.T.M. Palstra, G.J. Nieuwenhuys, J.A. Mydosh, K.H.J. Buschow, Phys. Rev. B 31 (1985) 4622.
[18] F. Wang, J. Zhang, Y.F. Chen, G.J. Wang, J.R. Sun, S.Y. Zhang, B.G. Shen, Phys. Rev. B 69 (2004) 094424.
[19] D. Givord, R. Lemaire, IEEE Trans. Magn. 10 (1974) 109.
[20] Z.W. Li, A.H. Morrish, Phys. Rev. B 55 (1997) 3670.
[21] L. Jia, J.R. Sun, J. Shen, Q.Y. Dong, F.X. Hu, T.Y. Zhao, B.G. Shen, Appl. Phys. Lett. 92 (2008) 182503.
[22] M. Rosca, M. Balli, D. Fruchart, D. Gignoux, E.K. Hlil, S. Miraglia, B. Ouladdiaf, P. Wolfers, J. Alloys Compd. 490 (2010) 50.
[23] J. Rodriguezcarvajal, Physica B 192 (1993) 55.
[24] O. Moze, W. Kockelmann, J.P. Liu, F.R. de Boer, K.H.J. Buschow, J. Magn. Magn. Mater. 195 (1999) 391.
[25] F.W. Wang, G.J. Wang, F.X. Hu, A. Kurbakov, B.G. Shen, Z.H. Cheng, J. Phys.: Condens. Matter 15 (2003) 5269.
[26] S. Fujieda, A. Fujita, K. Fukamichi, N. Hirano, S. Nagaya, J. Alloys Compd. 408 (2006) 1165.
[27] A. Fujita, S. Fujieda, K. Fukamichi, J. Magn. Magn. Mater. 321 (2009) 3553.
[28] L. Jia, J.R. Sun, F.W. Wang, T.Y. Zhao, H.W. Zhang, B.G. Shen, D.X. Li, S. Nimori, Y. Ren, Q.S. Zeng, Appl. Phys. Lett. 92 (2008) 101904.
[29] X.B. Liu, Z. Altounian, D.H. Ryan, J. Phys.: Condens. Matter 15 (2003) 7385.